

High- Q microfluidic cavities in silicon-based two-dimensional photonic crystal structures

Uwe Bog,¹ Cameron L. C. Smith,¹ Michael W. Lee,¹ Snjezana Tomljenovic-Hanic,¹ Christian Grillet,¹ Christelle Monat,¹ Liam O'Faolain,² Christian Karnutsch,^{1,*} Thomas F. Krauss,² Ross C. McPhedran,¹ and Benjamin J. Eggleton¹

¹Centre for Ultrahigh Bandwidth Devices for Optical Systems (CUDOS), School of Physics, University of Sydney, Sydney, NSW 2006, Australia

²School of Physics and Astronomy, University of St. Andrews, St. Andrews, Fife KY16 9SS, Scotland

*Corresponding author: c.karnutsch@physics.usyd.edu.au

Received June 10, 2008; revised August 18, 2008; accepted August 22, 2008;
posted August 28, 2008 (Doc. ID 97190); published September 26, 2008

We demonstrate postprocessed microfluidic double-heterostructure cavities in silicon-based photonic crystal slab waveguides. The cavity structure is realized by selective fluid infiltration of air holes using a glass microtip, resulting in a local change of the average refractive index of the photonic crystal. The microcavities are probed by evanescent coupling from a silica nanowire. An intrinsic quality factor of 57,000 has been derived from our measurements, representing what we believe to be the largest value observed in microfluidic photonic crystal cavities to date. © 2008 Optical Society of America

OCIS codes: 130.5296, 130.6010, 230.5298, 230.5750, 260.5740, 350.4238.

Optical microcavities in general, and two-dimensional photonic crystal (PhC) resonators in particular, represent a versatile platform for realizing various small-scale optical functionalities, such as lasers, optical switches, or sensors [1]. Design rules usually aim at generating high Q -factors and small modal volumes to trap light for a long time in a tiny fraction of space, which is crucial for high device performance and compactness. PhC microresonators are usually created by introducing a local inhomogeneity in the periodic lattice of air pores [1,2]. Such a “defect” typically consists of a permanent alteration of one or several hole dimensions and/or position. Achieving high- Q resonators through this approach however requires nanometer-scale fabrication accuracy [3], while the resulting resonator somewhat lacks tunability.

The infiltration of PhCs with fluids or polymers for realizing tunable optical devices or sensors was first suggested a decade ago [4] and experimentally demonstrated in both three-dimensional [5] and 2D [6–8] geometries. Later on, this idea was expanded through the concept of selective filling of individual air pores in a 2D PhC for creating various integrated functions and tunable photonic elements [9–11]. The actual breakthrough was achieved with recent advances in the development of microinfiltration techniques [12,13] and optofluidic integration [14] for locally infiltrating selected air pores. Whereas most of these demonstrations rely on the challenging infiltration of preexisting PhC cavities [6,8] or waveguide defects [14], we have shown that a PhC resonator could be directly created by infusing a fluid into any section of a uniform PhC waveguide [11,13]. This approach, which exploits the microfluidic equivalent of the double-heterostructure (DH) concept [15], relaxes the constraint on both the fabrication and infiltration accuracies for creating infused PhC microresonators. However, the first PhC cavities based on this concept exhibited Q -factors of only a few thousands [13],

which may preclude their use for sensing applications and lies well below the theoretical predictions [11].

In this Letter we demonstrate high- Q microfluidic DH cavities in silicon-based PhC slab waveguides. We present what we believe to be the highest Q -factor ever reported in the context of microfluidic cavity geometries in 2D PhC structures, 12 times higher than in our previous work [13], which was undertaken on chalcogenide waveguides. In addition to the different wetting properties of silicon and chalcogenide, the reduction of the hole diameter in the present study ($\varnothing=265$ nm instead of $\varnothing=380$ nm in chalcogenide) has implied successful improvement of our microtip-based infiltration technique. Besides the larger refractive index of silicon, the demonstration of higher Q -values is mainly attributed to the mature silicon PhC fabrication technology, resulting in reduced waveguide propagation losses. This allows us to show and discuss the high potential of this approach for resonance-based optofluidic sensing.

In this Letter a W0.9 PhC slab waveguide with a triangular lattice of air holes is investigated. The W0.9 configuration is a W1 waveguide—a PhC defect waveguide formed by omitting a row of holes in the Γ – K direction—where the PhC structure has been shifted inward such that the guide width is 0.9 times that of a W1. The PhC lattice exhibits a nominal periodicity of $a=410$ nm and a hole diameter of 265 nm ($0.646a$). It is fabricated into a 220-nm ($0.537a$)-thick suspended silicon membrane ($n_{\text{Si}}=3.52$). The dimensions of the PhC structure are $25\ \mu\text{m} \times 14\ \mu\text{m}$. The PhC waveguides are tailored to exhibit a photonic bandgap around 1400 nm for TE-like polarization. Their fabrication process is described in detail in [16].

The fluid infiltration (Fig. 1) starts with a glass microtip—tapered down to a diameter of 220 nm—being immersed into a fluid reservoir. When the tip is pulled out, fluid droplets remain attached

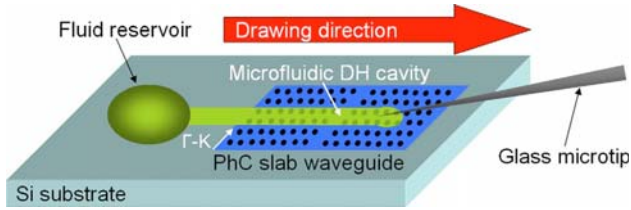


Fig. 1. (Color online) Schematic showing the fluid infiltration process. A glass microtip that has been immersed into a fluid is drawn across a PhC waveguide, creating a microfluidic DH cavity.

due to adhesive forces and the hydrophilic nature of the glass. These residues form a smaller reservoir as the tip is brought into contact with the sample surface close to the waveguide structure. By drawing a selected reservoir in a line across the PhC waveguide, the fluid enters the holes under the influence of capillary forces, leading to the formation of a microfluidic DH cavity. Different cavity widths can be realized by successively repeating this drawing process. To achieve accurate control the tip is mounted onto a piezoactuated three-axis translation stage (Thorlabs NanoMax). The infiltration process is monitored by using a high-magnification ($150\times$) optical microscope (Olympus BX61). The infiltrated liquid (Cargille immersion oil, type B) has a refractive index of $n_{\text{liquid}}=1.50$ at 1400 nm. Cavity widths of $3.3\ \mu\text{m}$ [Fig. 2(a)] and $16\ \mu\text{m}$ are investigated as typical representatives for a narrow and wide cavity.

The infiltration causes the original dispersion curve of the fundamental PhC waveguide mode to shift to lower frequencies while still remaining in the photonic bandgap of the surrounding uninfiltrated PhC [Fig. 2(b)]. This newly generated band structure exhibits modes that can propagate only inside the infiltrated area. This is due to the light now being confined in all spatial directions by either total internal reflection (orthogonal to the PhC plane), the photonic bandgap (in-plane perpendicular to the $\Gamma-K$ direction) [15]. In comparison to the W1 configuration, the fundamental waveguide mode of the W0.9 structure is

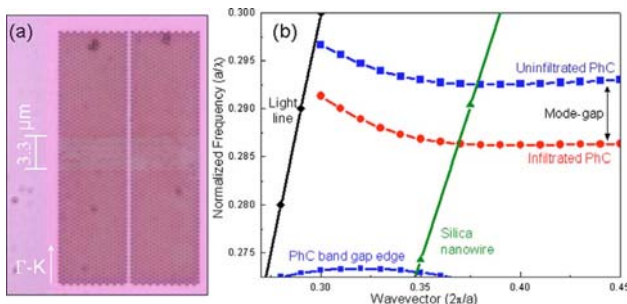


Fig. 2. (Color online) (a) Microscope picture ($150\times$ magnification) showing a microfluidic DH cavity of $3.3\ \mu\text{m}$ in width. The infiltration area appears as the region where the contrast between the holes and the PhC matrix is reduced. (b) Calculated dispersion relation of the fundamental mode of a W0.9 PhC waveguide, which is either uninfiltrated (rectangles) or infiltrated with a liquid of $n_{\text{liquid}}=1.5$ (filled circles). The line represents the dispersion curve of the silica nanowire used for evanescent coupling.

localized at higher frequencies and is further apart from the lower bandgap edge of the PhC [17]. The resulting mode-gap offered by the W0.9 makes it more promising for generating DH cavities, enabling a broader range of liquid refractive indices to be used, until the Q -factor becomes degraded by shifting the waveguide mode too close to the lower PhC bandgap edge [11].

The infiltrated DH cavities were investigated by evanescent coupling, bringing a silica nanowire into close proximity above the PhC waveguide [13]. The optical signal that is launched into the nanowire is TE polarized and delivered by a near-IR (NIR) super-continuum source (Fianium Femtopower 1060 SC450). The evanescent interaction between the PhC structure and the nanowire affects the spectral characteristics of the transmitted light, which is monitored using a high-resolution optical spectrum analyzer (Ando AQ6317B). The nanowire presents a waist diameter of $1.3\ \mu\text{m}$ and is shaped into an unclosed loop. The loop allows us to restrict the evanescent interaction to a localized area. All measurements are taken while the nanowire is not in contact with the PhC structure.

Figure 3 shows the transmission spectrum associated with the $3.3\ \mu\text{m}$ wide microfluidic DH cavity. Pronounced local minima are observed, attributed to Fabry–Perot (FP) modes of the microfluidic cavity, as the mode-gap effect causes the interfaces between the infiltrated and the uninfiltrated waveguides to act as highly reflective mirrors. The measured group velocities derived from the free spectral range between the FP modes are in good agreement with simulations (details will be published elsewhere [17]). The resonances exhibit measured Q -factors ranging between $Q_M=19,300$ [for resonance (1), transmission $T=0.88$] and $Q_M=36,300$ [resonance (4), $T=0.91$]. Taking the transmission T into account, the intrinsic Q -factor Q_{intr} is calculated by the first approximation coupled mode theory in the time domain to be $Q_{\text{intr}}=Q_M/T^{1/2}$. Hence, for resonances (1) and (4) intrinsic Q -factors of $Q_{\text{intr}}=20,810$ and $Q_{\text{intr}}=38,050$ are derived. This $3.3\ \mu\text{m}$ wide PhC cavity corre-

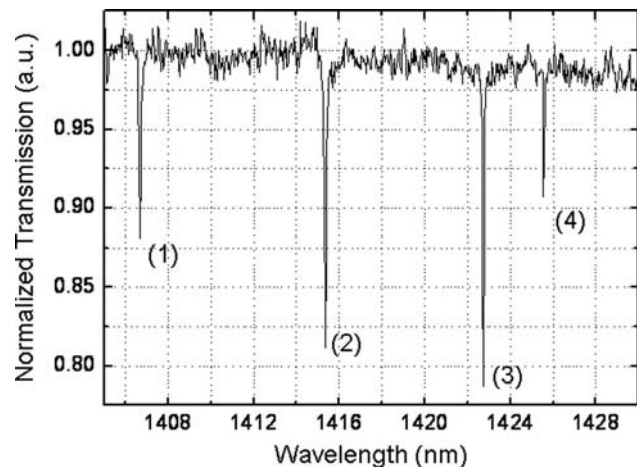


Fig. 3. Transmission spectrum while probing a microfluidic DH cavity of $3.3\ \mu\text{m}$ in width. The rightmost cavity mode (4) exhibits a measured Q -factor of $Q_M=36,300$.

sponds to a modal volume of $\sim 1.5 (\lambda/n)^3$ [11], showing the potential of generating high quality factors in very compact microfluidic devices.

Figure 4 shows the transmission spectrum when probing a $16 \mu\text{m}$ cavity. More spectral dips are observed, as expected in longer cavities that typically sustain an increased number of modes. The associated Q -factors are higher than for the shorter cavity, showing that the loss must be dominated by the reflection losses at the infiltrated–uninfiltrated interfaces. As an example, resonances (5) and (6) exhibit measured Q -factors of $Q_M=45,740$ and $Q_M=52,050$. The derived intrinsic Q -factors for these resonances are $Q_{\text{intr}}=50,430$ and $Q_{\text{intr}}=57,080$, respectively.

In contrast with early demonstrations of infused PhC cavities, where the Q -factor was typically degraded after the infiltration step [8], the high Q -factors presented here demonstrate that the DH cavity can be applied as a highly sensitive microfluidic sensor. PhC cavity band sensors typically exploit the resonance shift $\Delta\lambda$ that occurs when the refractive index of the analyte in the PhC holes changes by a value Δn . The shift of the waveguide band structure induced by the fluid infiltration, as calculated by plane-wave expansion, allows us to estimate a potential sensitivity $\Delta\lambda/\Delta n$ of 60 nm/RIU (refractive index unit). Considering the FWHM of the cavity resonance as the resolution limit, a minimum refractive index change of $\delta n_{\text{fluid}}=4.5 \times 10^{-4}$ could be detected by exploiting resonance (6) in Fig. 4. This value compares favorably with the values ($\delta n_{\text{fluid}}=0.002$) demonstrated in a previous work on PhC based sensors [6], although the ratio of the electromagnetic energy overlapping with the PhC holes appears to be limited to $\sim 6\%$ in our case, as estimated from the first-order approximation electromagnetic perturbation theory [18]. This overlap could be improved by engineering the cavity geometry.

In summary, we have demonstrated high Q -factors in postprocessed microfluidic photonic crystal double-heterostructure cavities. These cavities were created

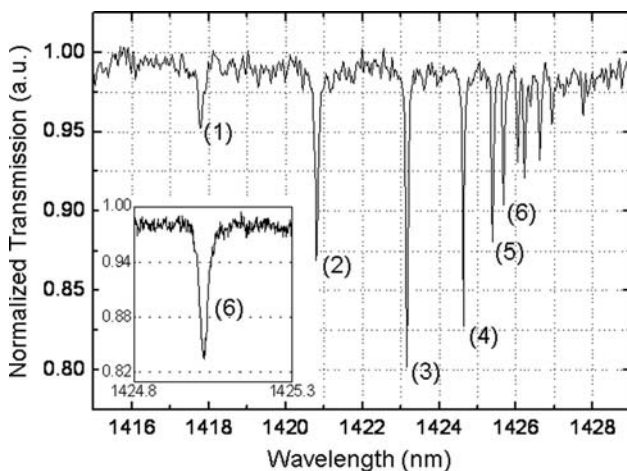


Fig. 4. Transmission spectrum while probing a $16 \mu\text{m}$ cavity. The measured Q -factors for the cavity modes (5) and (6) are $Q_M=45,740$ and $Q_M=52,050$. Inset, close-up view of resonance (6).

by infiltrating silicon-based photonic crystal slab waveguides, showing the possibility for realizing complex microfluidic structures in standard silicon chip technology. The high Q -factors measured show the potential for creating high-performance microfluidic devices on a wavelength-scale. An intrinsic Q -factor of 57,000 has been derived, sufficient for a wide range of applications in high-discrimination sensing, low-threshold microlasers, and quantum-electrodynamic studies.

The support of the Australian Research Council through its Federation Fellow, Centre of Excellence and Discovery grant programs is gratefully acknowledged. Additional acknowledgment is given to the support of the School of Physics, University of Sydney, through its Denison Foundation and the International Science Linkages (ISL) program by the Department of Education, Science, and Training (DEST) ISL DEST grant. The silicon samples were fabricated in the framework of the EU-FP6 funded ePIXnet Nanostructuring Platform for Photonic Integration (www.nanophotonics.eu).

References

1. K. Busch, S. Lölkes, R. B. Wehrspohn, and H. Föll, *Photonic Crystals-Advances in Design, Fabrication, and Characterization* (Wiley-VCH, 2004).
2. S. John, *Phys. Rev. Lett.* **58**, 2486 (1987).
3. T. Asano, B. S. Song, and S. Noda, *Opt. Express* **14**, 1996 (2006).
4. K. Busch and S. John, *Phys. Rev. Lett.* **83**, 967 (1999).
5. K. Yoshino, Y. Shimoda, Y. Kawagishi, K. Nakayama, and M. Ozaki, *Appl. Phys. Lett.* **75**, 932 (1999).
6. E. Chow, A. Grot, L. W. Mirkarimi, M. Sigalas, and G. Girolami, *Opt. Lett.* **29**, 1093 (2004).
7. S. W. Leonard, J. P. Mondia, H. M. van Driel, O. Toader, S. John, K. Busch, A. Birner, U. Gösele, and V. Lehmann, *Phys. Rev. B* **61**, R2389 (2000).
8. M. Loncar, A. Scherer, and Y. M. Qiu, *Appl. Phys. Lett.* **82**, 4648 (2003).
9. S. F. Mingaleev, M. Schillinger, D. Hermann, and K. Busch, *Opt. Lett.* **29**, 2858 (2004).
10. H. Takeda and K. Yoshino, *Phys. Rev. B* **67**, 073106 (2003).
11. S. Tomljenovic-Hanic, C. M. de Sterke, and M. J. Steel, *Opt. Express* **14**, 12451 (2006).
12. F. Intonti, S. Vignolini, V. Turck, M. Colocci, P. Bettotti, L. Pavesi, S. L. Schweizer, R. Wehrspohn, and D. Wiersma, *Appl. Phys. Lett.* **89**, 211117 (2006).
13. C. L. C. Smith, D. K. C. Wu, M. W. Lee, C. Monat, S. Tomljenovic-Hanic, C. Grillet, B. J. Eggleton, D. Freeman, Y. Ruan, S. Madden, B. Luther-Davies, H. Giessen, and Y.-H. Lee, *Appl. Phys. Lett.* **91**, 121103 (2007).
14. D. Erickson, T. Rockwood, T. Emery, A. Scherer, and D. Psaltis, *Opt. Lett.* **31**, 59 (2006).
15. B. S. Song, S. Noda, T. Asano, and Y. Akahane, *Nat. Mater.* **4**, 207 (2005).
16. J. Li, T. P. White, L. O'Faolain, A. Gomez-Iglesias, and T. F. Krauss, *Opt. Express* **16**, 6227 (2008).
17. C. L. C. Smith, U. Bog, S. Tomljenovic-Hanic, M. W. Lee, D. K. C. Wu, L. O'Faolain, C. Monat, C. Grillet, T. F. Krauss, C. Karnutsch, R. C. McPhedran, and B. J. Eggleton, *Opt. Express* **16**, 15887 (2008).
18. N. Mortensen, S. Xiao, and J. Pedersen, *Microfluid. Nanofluid.* **4**, 117 (2008).